J|A|C|S
ARTICLES
Published on Web 05/01/2002

Pulsed EPR Studies of Nonexchangeable Protons near the Mo(V) Center of Sulfite Oxidase: Direct Detection of the α-Proton of the Coordinated Cysteinyl Residue and Structural Implications for the Active Site

Andrei V. Astashkin,*,†,§,|| Arnold M. Raitsimring,*,†,|| Changjian Feng,† Jean L. Johnson,‡ K. V. Rajagopalan,‡ and John H. Enemark*,†,⊥

Department of Chemistry, University of Arizona, Tucson, Arizona 85721-0041, Department of Biochemistry, Box 3711, Duke University Medical Center, Durham, North Carolina 27710

Received June 25, 2001

Abstract: Pulsed electron nuclear double resonance (ENDOR) spectra of nonexchangeable protons in the vicinity of the Mo(V) center of the high pH (hpH) and low pH (lpH) forms of native chicken liver sulfite oxidase (SO) and recombinant human SO have been obtained and analyzed for the first time. The close similarity of the spectra for the chicken and human enzymes indicates that the structures of their molybdenum centers are essentially identical. For lpH SO, the closest nonexchangeable proton is found to be ~2.8 Å from the Mo atom. To more accurately determine the distance to this proton and facilitate its assignment, the C-band electron spin−echo envelope modulation (ESEEM) spectra of lpH SO were also analyzed. From the obtained distance and comparison with the X-ray structure, this closest nonexchangeable proton is assigned to the α-proton of the coordinated conserved cysteinyl residue (Cys185 in chicken, Cys207 in human). The closest Mo···H distance for the nonexchangeable protons of hpH SO is found to be ~3.3 Å. For the cysteinyl α-proton, such an increase in the Mo···H distance only requires a very small change in torsional angles. This study demonstrates that details of the enzyme structural rearrangements with pH can be monitored by ENDOR spectroscopy and suggests that a similar approach may be routinely used to probe the orientation of the coordinated cysteinyl residue in mutant forms of SO that are catalytically compromised.

Introduction

Sulfite oxidase (SO) is a physiologically vital enzyme that catalyzes the oxidation of sulfite to sulfate, the final step in sulfur metabolism in vertebrates. The crystal structure of chicken liver SO shows a novel five-coordinate distorted square pyramidal coordination geometry about the catalytic molybdenum center.[1] One of the equatorial ligands is the thiolate side chain of a cysteinyl residue that is conserved in all species and essential for catalytic activity.[2,3] The proposed mechanism for SO involves oxygen atom transfer followed by successive coupled electron/proton transfers that pass through the Mo(V) oxidation state, which is detectable by electron paramagnetic resonance (EPR).[4−6] Recently, we used pulsed EPR spectroscopy to investigate the Mo(V) center of chicken liver SO in H_2O and D_2O solutions. We showed that the phosphate-inhibited (Pi) form has a single monodentate rotationally disordered phosphate ligand.[7] Nearby, exchangeable protons have been investigated at pH 9.5 (high pH, hpH) and pH 7.0 (low pH, lpH) in order to establish the hydroxyl/water coordination structures.[6,8−10] We confirmed that the lpH form has a single hydroxyl proton with a large isotropic hyperfine interaction (hfi), lying in the equatorial coordination plane and, presumably, being weakly hydrogen-bonded to the S atom of the coordinated cysteinyl residue.[6,10] Refocused primary electron spin−echo envelope modulation (RP ESEEM) enabled nearby exchangeable protons in the hpH form to be detected for the first time, and simulation of the RP ESEEM spectrum favored two nearby protons with distributed hfi that were ascribed to an Mo^V−OH group with a strong H-bonding interaction to other nearby proton donors or to a coordinated H_2O ligand.[6]

|| Fax: 520 621-8407. E-mail: andrei@u.arizona.edu. E-mail: arnold@u.arizona.edu.
⊥ Fax: 520 626−8065. E:mail: jenemark@u.arizona.edu.
† University of Arizona.
‡ Duke University Medical Center.
§ On leave from the Institute of Chemical Kinetics and Combustion, Russian Academy of Sciences, Novosibirsk 630090, Russia.

(1) Kisker, C.; Schindelin, H.; Pacheco, A.; Wehbi, W. A.; Garrett, R. M.; Rajagopalan, K. V.; Enemark, J. H.; Rees, D. C. *Cell* **1997**, *91*, 973−983.
(2) Garrett, R. M.; Rajagopalan, K. V. *J. Biol. Chem.* **1996**, *271*, 7387−7391.
(3) George, G. N.; Garrett, R. M.; Prince, R. C.; Rajagopalan, K. V. *J. Am. Chem. Soc.* **1996**, *118*, 8588−8592.
(4) Rajagopalan, K. V. *Molybdenum and Molybdenum Containing Enzymes*; Coughlan, M., Ed.; Pergamon Press: New York, 1980; pp 243−272.
(5) Brody, M.; Hille, R. *Biochemistry* **1999**, *38*, 8 (20), 6668−6677.
(6) Astashkin, A. V.; Mader, M. L.; Pacheco, A.; Enemark, J. H.; Raitsimring, A. M. *J. Am. Chem. Soc.* **2000**, *122*, 5294−5302.
(7) Pacheco, A.; Basu, P.; Borbat, P.; Raitsimring, A. M.; Enemark, J. H. *Inorg. Chem.* **1996**, *35*, 7001−7008.
(8) Bray, R. C.; Gutteridge, S.; Lamy, M. T.; Wilkinson, T. *Biochem. J.* **1983**, *211*, 227−236.
(9) Lamy, M. T.; Gutteridge, S.; Bray, R. C. *Biochem. J.* **1980**, *185*, 397−403.
(10) Raitsimring, A. M.; Pacheco, A.; Enemark, J. H. *J. Am. Chem. Soc.* **1998**, *120*, 11263−11278.

The investigations described above were aimed at establishing the nature and binding geometry of the exchangeable ligands ($OH_{(2)}$, PO_4^{3-}) of the Mo(V) center. Another issue in discussing structure/function relationships in SO is the conformation of the coordinated cysteinyl ligand (Cys185 in the chicken amino acid sequence). It has been suggested[11] that the conformation of this residue can modulate the reactivity of the enzyme. In principle, the conformation of the cysteinyl ligand can be derived from the X-ray crystal structure of chicken liver SO.[1] This structure, however, was determined from single crystals grown in high concentration of sulfate at pH 7.8 starting with the fully oxidized Mo(VI) state of SO. Partial reduction of the Mo centers probably occurred in the X-ray beam during data collection,[1,12] so the exact oxidation state of the Mo center in the X-ray crystal structure is not known. On the other hand, EPR spectroscopy detects only the Mo(V) state. The lpH form is obtained at pH 7.0 in the presence of chloride; the hpH form is obtained a pH 9.5 in the absence of chloride. Intermediate pH values result in a mixture of the signals characteristic of lpH and hpH SO.[8] Having successfully addressed the nature of the *exchangeable* protons in these two forms of SO through pulsed EPR spectroscopy, we turn our attention to nearby *nonexchangeable* protons in order to obtain structural information about the conformation of the coordinated cysteinyl residue in the Mo(V) forms of SO.

During the past decade, several studies of the coordination of cysteinyl ligands in iron and copper proteins and their synthetic analogues by pulsed and continuous wave (CW) ENDOR and ESEEM have been reported.[13−16] The methodological aspects of these studies were useful for our investigation of the cysteinyl ligand to Mo in SO, but the magnitudes of the hyperfine interactions of the C_β-protons found in these previous studies could not be used directly here because of differences in the electronic structures of the respective metal centers. Therefore, as a background model for the prospective ENDOR/ESEEM investigation of the protons of the cysteinyl ligand in SO, we initially investigated *cis*,*trans*-(L-N_2S_2)$Mo^{V}O(SCH_2Ph)$ (L-$N_2S_2H_2$ = *N*,*N*′-dimethyl-*N*,*N*′-bis(mercaptophenyl)ethylenediamine), by pulsed EPR techniques.[17] In this system, the α-protons (methylene protons) of the benzyl thiolate ligand mimic the β-CH_2 protons of the cysteinyl ligand in SO. Using samples prepared with protonated and deuterated benzyl thiolate, we obtained the ENDOR spectra of these methylene protons and extracted their hfi parameters. The results for this model system were somewhat discouraging, because they indicated that the ENDOR lines of the β-CH_2 protons of SO are likely to be overlapped with those of other distant protons, and there may be little hope of detecting them without selective H→D isotopic substitution.

On the other hand, the X-ray structure of SO[1] shows that the C_α-proton of the cysteinyl ligand is only ∼2.96 Å from the Mo center, an exceptionally short distance that is considerably less than that to the C_β-protons, or to any other nonexchangeable protons. This C_α-proton should be detectable by ENDOR if the conformation of the coordinated cysteinyl residue in the Mo(V) states in frozen solution is not significantly different from that in the crystal structure. However, if the distance between the Mo(V) center and the C_α-proton were considerably larger than that in the crystal structure, then this proton would not be detected, and one could estimate the minimal conformational change required to "hide" the ENDOR lines of this C_α-proton. Therefore, we have performed pulsed ENDOR studies on the *nonexchangeable* protons of the lpH and hpH forms of chicken liver SO for direct comparison with one another and with the nearby proton environment that can be calculated from the X-ray crystal structure. In addition, since no X-ray structures are available for SO from sources other than chicken liver, we extended our pulsed ENDOR experiments to recombinant human SO so that the structures of the Mo sites in these two organisms can be compared. The results presented here suggest that the structure of the Mo site in human and chicken SO is well-conserved. In the ENDOR spectra of lpH SO, the features with the largest splting are attributed to the C_α-proton, as anticipated based on the X-ray structure. This assignment was facilitated by ESEEM experiments performed in the microwave (mw) C-band. In hpH SO, the distance to this proton has increased. Its resonances are masked by those of other distant protons and cannot be detected separately. The minimum conformational change of the cysteinyl ligand required to convert the X-ray crystal structure to that of the hpH form has been estimated. The results of this work provide a foundation for monitoring the conformation of the coordinated cysteinyl residue in mutant forms of SO that are catalytically compromised.

Experimental Section

Samples of highly purified chicken liver SO in D_2O and H_2O buffers in the lpH and hpH forms were prepared as previously described.[7,10] His-tagged recombinant human SO was purified from TP1000 cells containing pTG718.[18] After harvest, the cells were broken in the presence of a mixture of protease inhibitors supplied as EDTA-free protease inhibitor cocktail tablets (Roche Diagnostics). Chromatography on the NiNTA resin was carried out as described[18] and was followed by a final purification step on DE-52 using a gradient of sodium phosphate buffer, pH 7.8, from 50 to 350 mM containing 0.1 mM EDTA. EPR spectra of the lpH and hpH forms of His-tagged human SO were obtained using samples in buffers containing 100 mM Tris, 100 mM NaCl (pH 7.0, lpH), and 100 mM bis-Tris-propane (pH 9.5, hpH), respectively. The pH was adjusted by adding 6 M HCl. The protein was reduced with a 20-fold excess of sodium sulfite and immediately frozen in liquid nitrogen.

The Davies ENDOR[19] experiments were performed on a modified home-built X/P-band-pulsed EPR spectrometer[20] equipped with a cryogenic flow system and a pulsed ENDOR accessory.[21] The ESEEM experiments were performed on a home-built S/C-band-pulsed EPR spectrometer,[22,23] at a mw frequency of ∼4.7 GHz. The measurement temperature was ∼20 K.

(11) Izumi, Y.; Glaser, T.; Rose, K.; McMaster, J.; Basu, P.; Enemark, J. H.; Hedman, B.; Hodgson, K. O.; Solomon, E. I. *J. Am. Chem. Soc.* **1999**, *121*, 10035−10046.
(12) George, G. N.; Pickering, I. J.; Kisker, C. *Inorg. Chem.* **1999**, *38*, 2539−2540.
(13) Mouesca, J.-M.; Rius, G.; Lamotte, B. *J. Am. Chem. Soc*. **1993**, *115*, 4714−4731.
(14) Doan, P. E.; Fan, C.; Hoffman, B. M. *J. Am. Chem. Soc*. **1994**, *116*, 1033−1041.
(15) Dikanov, S. A.; Bowman, M. K. *J. Biol. Inorg. Chem*. **1998**, *3*, 18−29.
(16) Neese, F.; Kappl, R.; Hüttermann, J.; Zumft, W. G.; Kroneck, P. M. H. *J. Biol. Inorg. Chem*. **1998**, *3*, 53−67.
(17) Astashkin, A. V.; Mader Cosper, M.; Raitsimring, A. M.; Enemark, J. H. *Inorg. Chem*. **2000**, *39*, 4989−4992.
(18) Temple, C. A.; Graf, T. N.; Rajagopalan, K. V. *Arch. Biochem. Biophys.* **2000**, *383*, 281−287.
(19) Davies, E. R. *Phys. Lett. A* **1974**, *47*, 1.
(20) Borbat, P. P.; Raitsimring, A. M. Abstracts of 36th Rocky Mountain Conference on Analytical Chemistry, Denver, CO, 1994; p 94.
(21) Astashkin, A. V.; Raitsimring, A. M.; Kennedy, A. R.; Shokhireva, T. K.; Walker, F. A. *J. Phys. Chem. A* **2002**, *106*, 74−82.

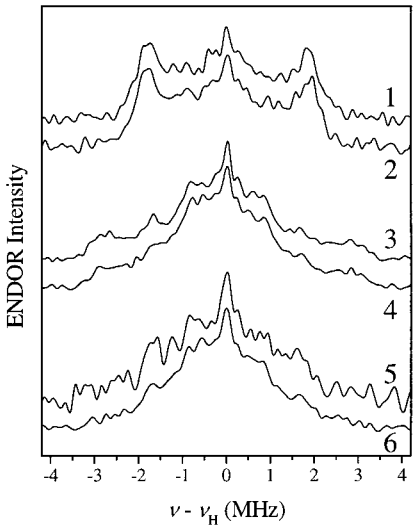

Figure 1. Davies ENDOR spectra of the lpH form of chicken (traces 1, 3, and 5) and human (traces 2, 4, and 6) SO in the H_2O buffer. Traces 1 and 2, B_o= 3365 G (about g_3). Traces 3 and 4, B_o= 3418 G (about g_2). Traces 5 and 6, B_o= 3439 G (about g_1). Experimental conditions: mw pulses, 120 (180°), 60 (90°), and 120 ns (180°); interval T between the first and second mw pulses, 40 μs; interval τ between the second and third mw pulses, 400 ns; RF pulse duration (180°), 8 μs; microwave frequency, ν_{mw} = 9.449 GHz.; temperature, ~ 20 K.

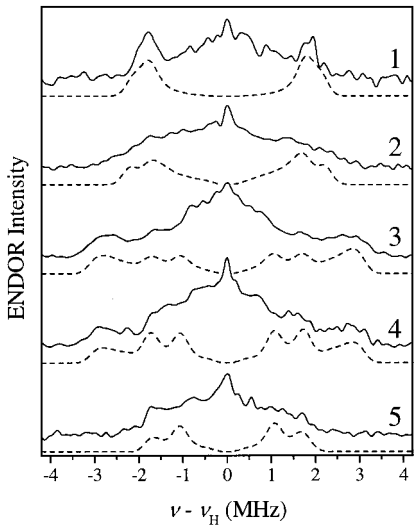

Figure 2. Solid traces 1 through 5, experimental Davies ENDOR spectra of the lpH form of chicken SO in the D_2O buffer, detected at B_o= 3365 (about g_3), 3390, 3418 (about g_2), 3429, and 3439 G (about g_1), respectively. Experimental conditions as in Figure 1. Dashed traces with the same numbers, calculated Davies ENDOR spectra with contributions of the three closest protons taken into account (see text and Figure 3). The **g** tensor orientation used in the calculation is shown in Figure 5.

The ENDOR spectra of chicken and human SO obtained in buffered H_2O solutions were virtually identical (see Figure 1). For this reason, and because of the limited amount of human SO available for these experiments, the experiments in D_2O solution were performed for chicken SO only.

Results and Discussion

EPR Spectra of lpH and hpH SO. As determined earlier[8,9,24,25] and confirmed by our measurements, the EPR spectra of chicken and human SO are similar and characterized by the following principal g values: $g_1 \approx 1.966$, $g_2 \approx 1.972$, and $g_3 \approx 2.004$ for the lpH form; and $g_1 \approx 1.953$, $g_2 \approx 1.964$, and $g_3 \approx 1.988$ for the hpH form. The subscripts at the principal g values correspond to the principal axes *1*, *2*, and *3* of the **g** tensor. In our notation, the principal g values g_1, g_2, and g_3 correspond, respectively, to g_3, g_2, and g_1 used elsewhere.[9] The notation was changed to avoid an unusual and confusing correspondence between the axes of the molecular coordinate frame *XYZ* and the g frame *123*, in which axis *3* would correspond to *X*; and *1*, to *Z*.

ENDOR Spectra of lpH SO. Figure 1 shows the Davies ENDOR spectra of chicken and human lpH SO obtained near the turning points of the EPR spectrum. The strongly coupled exchangeable protons give ENDOR signals outside the spectral range shown in this Figure.[10] The virtual identity of the ENDOR spectra of chicken and human SO indicates nearly identical structures for their Mo sites, as would be expected from the strong sequence homology for the two enzymes and the conserved sequence near the essential coordinating cysteine residue (Cys185 in chicken; Cys207 in human).[1]

To eliminate the contribution of exchangeable protons, the Davies ENDOR spectra of chicken SO in D_2O buffer were recorded (see Figure 2). Spectra 1, 2, and 3 shown in Figure 1 are similar to, respectively, spectra 1, 3, and 5 in Figure 2 (solid traces) recorded near the EPR turning points, which indicates that no nearby exchangeable protons contribute to this spectral region. In ENDOR spectrum 1 (Figure 2) recorded at g_3, the outer spectral lines have a splitting of ~3.7 MHz. At g_2 (spectra 3 and 4), the largest splitting between the spectral features is about 6 MHz. At g_1 (spectrum 5) the spectrum has a tent-like shape, with the edges corresponding to a splitting of ~3.45 MHz. It follows from Figure 2 that the 6 MHz splitting near g_2 is actually the largest observed splitting for the nonexchangeable protons in lpH SO.

In principle, tracing the variation of the ENDOR spectral shapes associated with a given proton with magnetic field B_o (i.e., across the anisotropic EPR spectrum) enables the hfi parameters for that proton to be unambiguously determined.[26] Such an approach requires the spectral lines of the proton in question to be resolved, at least at most $B_o$values, from the lines of other protons. In the ENDOR spectra of lpH SO, the only unique and potentially assignable feature is the pair of lines/shoulders with the largest splitting that attains its maximum value of ~6 MHz at g_2. However, this feature is only partly traceable across the EPR spectrum; its splitting decreases toward g_1 and g_3, where it begins to merge with the features of numerous more distant protons that are not well-resolved. In such a situation, we cannot undertake a full formal analysis of the orientation dependence of the ENDOR spectra, and we have to restrict ourselves to the analysis of the largest ENDOR splitting only and of that part of its orientation dependence that can be traced.

(22) Astashkin, A. V.; Kozliyuk V.; Raitsimring, A. M. Abstracts of 40th Rocky Mountain Conference on Analytical Chemistry, Denver, CO, 1998, Additional materials.
(23) Astashkin, A. V.; Raitsimring, A. M.; Walker, F. A. *Chem. Phys. Lett.* **1999,** 306, 9−17.
(24) Kessler, D. L.; Rajagopalan, K. V. *J. Biol. Chem.* **1972**, *247*, 6566−6573.
(25) George, G. N.; Rajagopalan, K. V. Unpublished results.
(26) Hoffman, B. M.; Gurbiel, R. J.; Werst, M. M.; Sivaraja, M. In *Advanced EPR: Applications in Biology and Biochemistry*; Hoff, A. J., Ed.; Elsevier: Amsterdam, 1989; pp 541−591.

As a first step in the data interpretation, we may use a point dipole approximation, assuming all the spin density to be localized on Mo (see Appendix 1) and neglecting the contribution of the isotropic hfi (see discussion below). Under these assumptions, the largest observed splitting (~6 MHz) corresponds to the orientation of $\mathbf{B}_o$ along the Mo···H radius vector $\mathbf{R}_{MoH}$. The anisotropic hfi constant $T_\perp$ is one-half of this maximal splitting, about −3 MHz, and the Mo···H distance can be estimated from $T_\perp$,

$$T_\perp = -gg_n\beta\beta_n/hR^3_{MoH} \quad (1)$$

where g and g_n are, respectively, the electronic and nuclear g factors; β and β_n are the Bohr magneton and the nuclear magneton; and h is Planck's constant. Using eq 1 with $T_\perp \approx -3$ MHz gives $R_{MoH} \approx 2.97$ Å. After correcting for spin density delocalization from Mo to the ligands, this distance is estimated to be ~2.9 Å (see Appendix 1). The values of the largest ENDOR splittings observed at g_1 and g_3 impose a restriction on the largest R_{MoH} for the nonexchangeable protons responsible for the outer features in the ENDOR spectra: $R_{MoH} \leq 3.6$ Å, as calculated from the 3.45 MHz splitting observed at g_1.

To understand which amino acid residues could provide such nearby nonexchangeable protons, we have analyzed the single-crystal X-ray structural data for chicken liver SO available in the protein database[27] (entry 1SOX). As mentioned in the Introduction, the single-crystal samples of SO were obtained at pH 7.8 in high sulfate concentration.[1] Although these conditions differ from those for obtaining the lpH and hpH forms of the Mo(V) state of SO, the X-ray crystal structure should provide background guidance for assigning the 6 MHz splitting to a particular proton or group of protons.

The positions of nearby nonexchangeable protons with respect to Mo were calculated from the coordinates of the carbon atoms obtained from the X-ray structure, taking into account the appropriate hybridization geometry at each carbon atom (see Appendix 1). The closest nonexchangeable proton is the C_α-proton of coordinated Cys185 ($R_{MoH} \approx 2.96$ Å, see Figure 3). The C_β-protons of Cys185 are at significantly greater distances (3.54 and 4.41 Å), and the maximum possible splittings associated with them are ~3.6 and 1.8 MHz, respectively. Of the other nearby (nonliganding) residues, only Arg138 has one of its γ-protons within 3.3 Å of Mo (see Figure 3). In the following analysis, we will adopt a conservative approach and assume minimal changes of the Mo structural environment from that found by X-ray crystallography upon changing the sample pH and the oxidation state of the Mo center. Therefore, we will not consider protons of nonliganding residues (e.g., Arg138) as candidates for explaining the 6 MHz splitting in the ENDOR spectra.

The analysis of all formally possible conformations of the cysteinyl ligand shows that the possible distance from Mo to the C_α-proton is confined within the range of 2.2−5.6 Å. For the C_β-protons, on the other hand, the possible distance is within the range of 3.1−4.4 Å. Thus, the distance $R_{MoH} \approx 2.9$ Å, estimated for the closest nonexchangeable proton in lpH SO, is well within the range of possible distances to the C_α-proton, and is, in fact, virtually indistinguishable (see Appendix 1) from

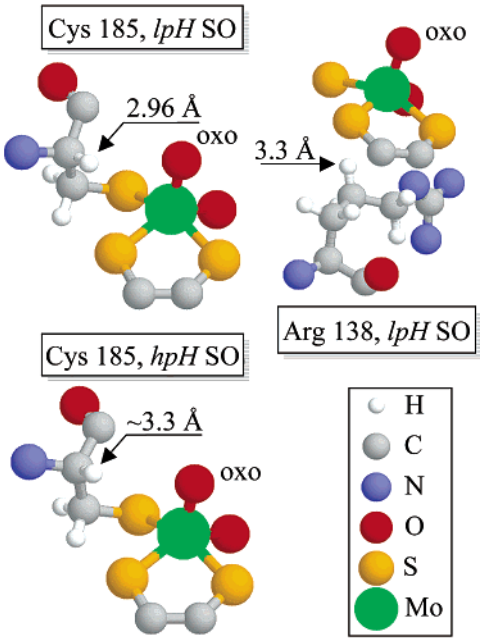

Figure 3. Geometry of Cys185 (top left) and Arg138 (top right) residues and their location with respect to the Mo center of chicken SO taken from the X-ray crystal structure.[1] The conformation of Cys185 in lpH SO found here by ENDOR is virtually indistinguishable from that derived from the X-ray structure. Bottom, suggested structure for the hpH SO obtained by two consecutive 15° rotations, around $C_\alpha-C_\beta$ and $C_\beta-S_\gamma$ bonds of Cys185. The distances to the closest protons are indicated. Only part of the pyranopterin ligand is shown.

the $R_{MoH} \approx 2.96$ Å estimated for this proton from the X-ray structure. This distance is smaller than the minimum possible distance to the C_β-protons. However, the C_β-protons may have appreciable isotropic hfi constants, and we next consider the possibility of assigning the 6 MHz splitting in the ENDOR spectra to these protons.

Of the various relevant systems studied by ENDOR that can give information on isotropic hfi constants of the cysteinyl C_β-protons, the one most closely related to the Mo center of SO is a model complex with Mo(V) ligated by a benzyl thiolate ligand.[17] In that work, we found that the torsional angles of the Mo−S−CH_2 fragment are distributed over wide limits, and the ENDOR spectral shapes of the methylene protons could be successfully simulated without taking the isotropic hfi into account. Although we cannot exclude that those spectra could also be simulated by including the conformation-dependent isotropic hfi, the conclusion about a wide distribution of torsional angles will also stand in this case. An important result of the model work[17] relevant to the current discussion for lpH SO is that the width of the ENDOR spectra did not exceed 4 MHz, which limits the possible estimates of the largest isotropic hfi to a value not exceeding ~2 MHz. This value would occur when one of the C_β-protons of SO becomes most distant from Mo (~4.4 Å).

Other estimates of the isotropic hfi constants of cysteine C_β-protons in SO and their dependence on the cysteine conformation can be obtained by invoking analogies with γ-protons in π-centered hydrocarbon radicals,[28,29] C_β-protons in S-centered cysteine radicals,[30] cysteine C_β-protons in iron−sulfur centers,[13−15] and the Cu center in N_2O reductase.[16] All of these estimates give a maximum isotropic hfi of ~3 MHz. In addition, quantum-chemical calculations of π-centered radicals predict that this

(27) Berman, H. M.; Westbrook, J.; Feng, Z.; Gilliland, G.; Bhat, T. N.; Weissig, H.; Shindyalov, I. N.; Bourne, P. E. *Nucleic Acids Res.* **2000**, *28*, 235−242, <http://www.rcsb.org/pdb>.

maximal hfi constant would correspond to a so-called W conformation, when the γ-proton is at the largest possible distance from the unpaired electron.[28,29] The hfi data on the cysteinyl C_β-protons in iron−sulfur centers[13−15] are in a general agreement with this conclusion. One should, however, be very cautious about such estimates, since they are based on systems that have electronic structures quite different from that studied here. Most likely, the ∼3 MHz isotropic hfi is somewhat overestimated, and thus, it is in qualitative agreement with ∼2 MHz estimated above for the model Mo complex with a benzyl thiolate ligand.[17] Even for the maximum estimated isotropic hfi of ∼3 MHz, the C_β-proton in the X-ray structure that is most distant from the Mo position (4.4 Å) can give an ENDOR splitting of no more than 4.9 MHz, considerably less than the 6 MHz obtained at g_2.

The minimum isotropic hfi is expected when a C_β-proton is near its closest approach to the Mo center. The value for the minimum constant is not very well defined. The expected range is from ∼0 (as obtained from the hydrocarbon analogy[28,29]) to ∼1 MHz (as found in iron−sulfur complexes[13−15]). In the extremely unlikely case of the minimum a_{iso} being ∼1 MHz and the C_β-proton being at the closest possible distance to Mo (3.1 Å), the maximum ENDOR splitting would be ∼6 MHz, similar to that obtained at g_2. The minimum angle of rotation around the $C_\beta-S_\gamma$ bond required to move one of C_β protons in SO to such a position from that calculated from the X-ray structure is ∼66°.

The above considerations show that the assignment of the 6 MHz splitting observed at g_2 to a C_β-proton of the coordinated cysteinyl residue (instead of the C_α one) cannot be completely ruled out on the basis of the value of the splitting only. On the other hand, this problem ultimately boils down to accurate evaluation of the anisotropic hfi of the proton responsible for this splitting. This could be achieved by accurately simulating the ENDOR spectra taken at various positions of the EPR spectrum if the complete ENDOR features attributable to this proton could be somehow separated from the lines of all other protons. This, however, is not the case, and therefore, it is not surprising that our trial ENDOR simulations (not shown, but similar to those described below and in Appendix 2) aimed at distinguishing between $T_\perp \approx -3$ MHz (C_α-proton at the distance of ∼2.9 Å) and $T_\perp \approx -2.5$ MHz (C_β-proton at the shortest possible distance of ∼3.1 Å that, in addition, has an isotropic hfi constant of ∼1 MHz) did not result in an unequivocal assignment. This is in part due to the rather small difference in the anisotropic hfi constants of these two protons.

To address this ambiguity, we turned our attention to the primary and four-pulse ESEEM spectra in which the up-frequency shift, $\Delta\nu_\sigma$, of the sum combination line (ν_σ) from the exact double Zeeman frequency of protons ($2\nu_H$) is proportional to the second power of $T_\perp$. For example, in an orientationally disordered system,[31]

$$\Delta\nu_\sigma \approx \frac{9T_\perp^2}{16\nu_H} \qquad (2)$$

If the ESEEM experiment is performed in X-band (mw frequency $\nu_{mw} \sim 9.5$ GHz, $B_o \sim 3450$ G, $\nu_H \sim 14.7$ MHz), the values of $\Delta\nu_\sigma$ expected for protons with $T_\perp \approx -3$ MHz and −2.5 MHz are, respectively, ∼0.34 and 0.24 MHz. Resolving such splittings in the ESEEM spectra requires rather long accumulation times, because the time domain data should be collected over a very long time interval (at least 10 μs) and with very small increments in pulse separations (∼10 ns) in order to avoid frequency aliasing. On the other hand, if the experiment is performed at lower mw frequencies/magnetic fields, $\Delta\nu_\sigma$ increases in proportion to $1/\nu_H$. In addition, as we already discussed in detail elsewhere,[23] the experiments at lower mw frequencies offer the advantages of increased ESEEM amplitude (specifically, for weakly coupled protons) and reduced data accumulation time. The mw frequency, however, should still be high enough to keep the proton in a "weak interaction region" and possibly far from the Zeeman/hfi cancellation, to avoid unnecessary complications in the subsequent interpretation of spectra. Our preliminary estimates showed that the mw frequencies optimal for such measurements are in the range of 4−5 GHz.

Therefore, the ESEEM experiments with a protonated sample of chicken lpH SO were performed at $\nu_{mw} = 4.747$ GHz and $B_o = 1715$ G, which corresponded to the maximum of the field-sweep ESE spectrum, and to $\nu_H \approx 7.3$ MHz. The two-pulse ESE field sweep spectrum collected with mw pulses of 10-ns duration has shown the width of 27 G at the half-height level. This width is considerably smaller than that observed in the X band (∼60 G), because it is mainly determined by the g factor anisotropy. The $\pi/2$ mw pulses of 10 ns ensured a spectrum excitation range of ∼8 G. In addition, the large hfi constant of the nearby exchangeable proton (∼10 G)[8] gave an effective increase of this range to ∼18 G, that is, to a value comparable with the total width of the EPR spectrum. As a result, the ESEEM spectra collected at the maximum of the EPR spectrum virtually corresponded to a completely orientationally disordered situation, and therefore, eq 2 could be used to analyze the data. In the primary ESEEM experiments, the shifted ν_σ line due to the cysteinyl protons could not be resolved from that of distant matrix protons, because the spectral resolution was limited by a rather short transverse relaxation time, $T_2 \sim 0.8$ μs. Therefore, we performed four-pulse experiments in which the spectral resolution is limited by the longitudinal relaxation time, $T_1 \gg T_2$. Figure 4 shows an example of a four-pulsed ESEEM spectrum of lpH SO in which the shifted ν_σ line of a cysteinyl proton is clearly observed. The shift $\Delta\nu_\sigma$ in this spectrum is ∼0.8 MHz. Substituting this shift into eq 2, one obtains the value of the anisotropic hfi constant, $T_\perp \approx -3.2$ MHz, which is in the range of possible constants for the C_α-proton. On the other hand, for a C_β-proton at the shortest possible distance ($T_\perp \approx -2.5$ MHz), the shift $\Delta\nu_\sigma$ would be ∼0.48 MHz, almost 1.7 times smaller than that observed in the experiment.

Thus, we may conclude that the largest ENDOR splitting observed at g_2 belongs to the cysteinyl C_α-proton. The outer features of the ENDOR spectra recorded at g_1 and g_3 can also have contribtions from one C_β-proton of Cys185 and one C_γ-proton of Arg138 (chicken numbers) that are located at distances

(28) Ellinger, Y.; Rassat, A.; Subra, R.; Berthier, G. *J. Am. Chem. Soc*. **1973**, *95*, 2372−2372.
(29) Zhidomirov, G. I.; Schastnev, P. V.; Chuvylkin, N. D. *Quantum Chemical Calculations of Magnetic-Resonance Parameters*; Nauka: Novosibirsk, 1978.
(30) Matsuki, K.; Hadley, J. H., Jr.; Nelson, W. H.; Yang, C.-Y. *J. Magn. Reson. A* **1993**, *103*, 196−202.
(31) Dikanov, S. A.; Tsvetkov, Yu. D. *Electron Spin−Echo Envelope Modulation (ESEEM) Spectroscopy*; CRC Press: Boca Raton, FL, 1992.

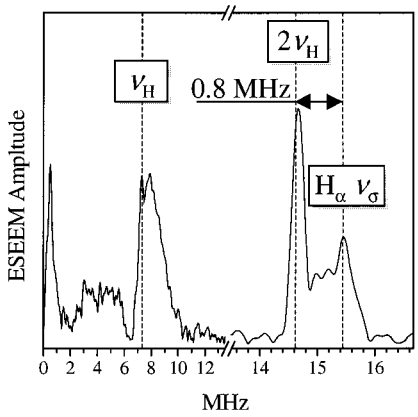

Figure 4. Four-pulse ESEEM spectrum of lpH SO in the H_2O buffer obtained at $\nu_{mw} = 4.747$ GHz, $B_o = 1715$ G, $\tau = 380$ ns. All mw pulse durations were 10 ns. Temperature, ~20 K. The shifted ν_σ line of the cysteinyl C_α-proton is marked "H_α ν_σ".

of 3.54 and 3.3 Å, respectively. To further check the reasonability of this assignment and to obtain the information on the orientation of the **g** tensor axes relative to the Mo complex, we have performed the ENDOR simulations with variation of the **g** tensor orientation in the molecular frame. The molecular frame *XYZ* was defined as follows: axis *Z* was directed along the Mo═O bond, *X* ($\perp Z$) was in the plane defined by the Mo═O bond, and the Mo−OH bond, and *Y* was perpendicular to both *X* and *Z* (and roughly pointing in the direction of the bond between Mo and the S atom of the cysteine ligand). The orientation of the *g* frame *123* was defined by Euler angles ψ, θ, and φ, which are the angles for three consecutive rotations around, respectively, *3*, newly obtained *1* and newly obtained *3*. The situation with all the of angles equal to 0 corresponds to the orientation of *1* // *X*, *2* // *Y* and *3* // *Z*. The simulation procedure is described in Appendix 2.

In the previous work,[10] the hfi tensor of the nearby exchangeable OH proton was determined, and it was noted that the large isotropic hfi constant of that proton indicates that the OH bond is approximately in the plane of the molybdenum d_{xy} orbital carrying the unpaired electron. In such a situation, the local symmetry requires that the main axis of the anisotropic hfi tensor of the OH proton is also in the d_{xy} plane. Since the main axis of the anisotropic hfi was found to be virtually parallel with axis *1* of the **g** tensor,[10] we may conclude that axis *1* is approximately in the *XY* plane. Therefore, in our ENDOR simulations, we assumed $\varphi = 0°$.

The ENDOR simulations reproduce the largest splittings in the spectra of lpH SO (see Figure 2) if the **g** tensor orientation in the molecular coordinate frame is described by $\psi \approx 10° \pm 5°$, $\theta \approx 30° \pm 10°$, and $\varphi \approx 0°$. For the convenience of the reader, we also express this orientation in another popular Euler angles system: $\alpha \approx -80° \pm 5°$, $\beta \approx 30° \pm 10°$, and $\gamma \approx 90°$, where α, β, and γ are the angles for three consecutive rotations around, respectively, *3*, newly obtained *2* and newly obtained *3*. The molecular axes and the **g** tensor orientation obtained are shown in Figure 5. The values of a_{iso} and $T_\perp$ for the cysteine C_α-proton used in the simulation presented in Figure 2 are −0.3 and −3.3 MHz, respectively. This value of $T_\perp$ is very close to that obtained above from the ESEEM measurements and translates into the distance $R_{MoH} \approx 2.8$ Å for $\rho_{Mo} = 0.85$ (with a distance correction factor of 0.975; see Appendix 1), close to $R_{MoH} \approx 2.96$ Å found from the X-ray structure. Such a

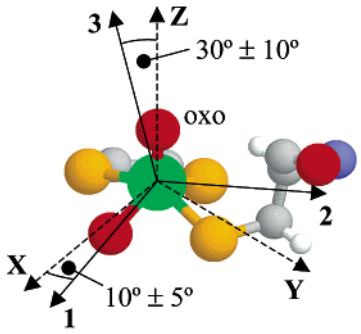

Figure 5. The orientation of the **g** tensor axes *1*, *2*, and *3* with respect to the molecular axes *X*, *Y* and *Z*, as used in the calculation of spectra shown in Figure 2. The Euler angles describing the orientation of the **g** tensor axes are $\psi \approx 10° \pm 5°$, $\theta \approx 30° \pm 10°$, and $\varphi \approx 0°$.

difference in R_{MoH} is at the margin of distinguishability (see Appendix 1) and can be achieved by a ≤6° rotation around the cysteine $C_\alpha - C_\beta$ bond followed by a ≤6° rotation around the $C_\beta - S_\gamma$ bond. Since such a structural change is very insignificant, we may, to the first approximation, consider the geometry of the cysteine ligand in lpH SO to be similar to that found by X-ray crystallography (see Figure 3). The isotropic hfi value of about −0.3 MHz translates into a spin density at a proton of $\sim 2 \times 10^{-4}$.

The values of $T_\perp$ for the C_β-proton of Cys185 and the C_γ-proton of Arg138 taken into account in the simulation were estimated using a point dipole approximation (−1.78 and −2.2 MHz, respectively). Spectra 1, 3, 4, and 5 in Figure 2 could be successfully simulated assuming a zero isotropic hfi constant for the cysteine C_β-proton. However, to fit the overall width of the ENDOR spectrum 2, we also had to introduce for this proton $a_{iso} \approx 1$ MHz. This isotropic hfi constant is in the range of values discussed above for such a proton. The simulated spectra 1 and 3−5 in Figure 2 practically did not depend on whether $a_{iso} = 0$ MHz or $a_{iso} \approx 1$ MHz was used for the cysteine C_β-proton (at least for the Euler angles $\psi \approx 10° \pm 5°$, $\theta \approx 30° \pm 10°$, and $\varphi \approx 0°$).

The significant departure of the **g** tensor axes in lpH SO from the molecular axes *X*, *Y*, and *Z* obtained in our calculations is in general agreement with the results of other EPR studies of low-symmetry oxo-Mo(V) centers.[32] Axis *2* of the **g** tensor for SO obtained in this work is at an angle of only ~30° with the direction to the cysteine C_α-proton. With such an arrangement, the orientations of the other two axes could not be accurately established if we did not fix $\varphi = 0°$, which is an approximate model restriction obtained from considering the hfi parameters of the nearby exchangeable proton (see above). Axis *1* of the **g** tensor, thus, lies by definition in the equatorial plane. The estimated value $\psi \approx 10°$ shows that this axis points approximately in the direction of the oxygen of the OH ligand (Figure 5), which is in agreement with our previous ESEEM investigation of the proton of the Mo−OH group in lpH SO.[10] The estimated value $\theta \approx 30°$ shows that the Mo orbital carrying the unpaired electron is not a pure d_{xy} orbital (a result one could expect a priori from the distroted geometry of the complex). Therefore, the assumption of $\varphi = 0°$ used in the calculations cannot be strictly valid, and one may expect some departure of axis *1* from the *XY* plane. The scale of the possible departure is

(32) Mabbs, F. E.; Collison, D. *Electron Paramagnetic Resonance of d Transition Metal Compounds*; Elsevier: Amsterdam, 1992.

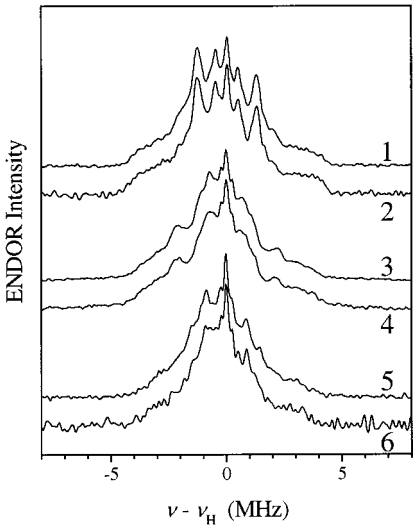

Figure 6. Davies ENDOR spectra of the hpH form of chicken (traces 1, 3, and 5) and human (traces 2, 4, and 6) SO in H_2O buffer. Traces 1 and 2, $B_o = 3396$ G (about g_3). Traces 3 and 4, $B_o = 3437$ G (about g_2). Traces 5 and 6, $B_o = 3460$ G (about g_1). Experimental conditions as in Figure 1.

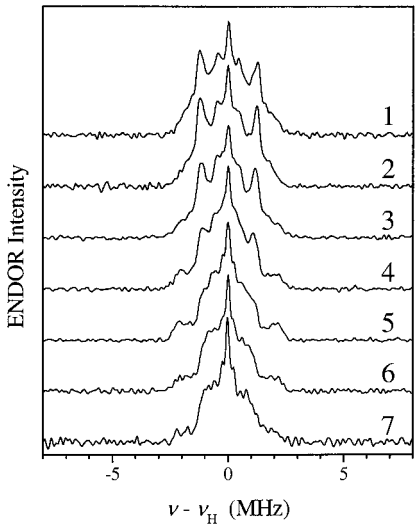

Figure 7. Traces 1 through 7, Davies ENDOR spectra of the hpH form of chicken SO in D_2O buffer, detected at $B_o = 3396$ (about g_3), 3405, 3415, 3425, 3437 (about g_2), 3448, and 3460 G (about g_1), respectively. Experimental conditions as in Figure 1.

given, in fact, by the nonzero value of θ that reflects the asymmetry of the complex.

ENDOR Spectra of hpH SO. Figure 6 compares the Davies ENDOR spectra of chicken and human hpH SO in H_2O obtained near the turning points of the EPR spectrum. As was observed for lpH SO, the spectra of chicken and human SO are virtually identical, which indicates that the positions of both the nearby exchangeable and nonexchangeable protons at the Mo site are conserved.

The ENDOR spectra of hpH SO in buffered D_2O solution are shown in Figure *7*. All spectra exhibit the same features, shoulders with a splitting of ~4.4 MHz and a pair of features with a smaller splitting (2.2−2.5 MHz) that look like peaks for the observation positions between g_3 and g_2, but rather like shoulders between g_2 and g_1. As a whole, the ENDOR spectra of hpH SO show considerably weaker dependence on the observation position than the spectra of lpH SO. A striking difference compared to the spectra of lpH SO is that the maximum observed splitting for hpH SO is 4.4 versus 6 MHz for lpH SO.

The broad shoulders with a splitting of ~7 MHz observed in the spectra of Figure 6 are not seen in Figure 7, which indicates that they belong to exchangeable protons. This 7 MHz splitting correlates with the maximum $T_\perp$ value (~ 7.3 MHz) determined earlier by ESEEM for the exchangeable Mo−OH protons in hpH chicken SO,[6] and therefore, these shoulders are attributed to such protons. The close similarity of these features in the spectra of chicken and human SO (Figure 6) suggests that human SO also has two nearby exchangeable protons with distributed hfi that can be ascribed to a Mo^V−OH group with a strong H-bonding interaction to other nearby proton donors or to a coordinated H_2O ligand.[6]

The maximum splitting of 4.4 MHz in the ENDOR spectra of hpH SO corresponds to the minimum distance $R_{MoH} \approx 3.3$ Å, as estimated for $\rho_{Mo} = 1$ and zero isotropic hfi. The average distance correction factor of 0.99 derived for hpH SO ($\rho_{Mo} \approx 0.9$) in Appendix 1 virtually does not change this value. The differences between the R_{MoH} value in hpH SO and those in lpH SO and in the X-ray structure are well above the limits of distinguishability discussed in Appendix 1. It is straightforward to conclude that some structural variations occurred at the Mo site of SO upon raising the pH. Notably, some change of geometry of the Cys185 residue has taken place. It seems unreasonable to assume any major changes in the protein folding, and the total structural alterations are probably rather small. Indeed, the shift of the C_α-proton of Cys185 from the X-ray value of $R_{MoH} \approx 2.96$ Å to $R_{MoH} \approx 3.3$ Å can be achieved by two consecutive rotations of ~15° around $C_\alpha-C_\beta$ and $C_\beta-S_\gamma$ bonds of the cysteine (in the directions opposite to those assumed for the lpH SO), which is a very subtle change in the cysteine geometry, indeed. The resulting hypothetical structure of the Mo−Cys fragment in the hpH SO is shown in Figure 3 (bottom structure).

The fact that the spectra of hpH SO look rather similar at any $\mathbf{B}_o$ orientation indicates that there are several protons located at distances ~3.3 Å but at various angular positions in the molecular frame. Two such protons are the C_α-proton of Cys185 and the C_γ-proton of Arg138 that were mentioned previously. The ~15° rotation around the $C_\beta-S_\gamma$ bond of the cysteine discussed above will also bring one of the C_β-protons of Cys185 to a distance of ~3.4 Å, very close to that required for the observed ENDOR splittings. Such a variation in the geometry of Cys185 with pH could reflect a slightly different general protein structure around the molybdenum center at pH 9.5, as compared with that at pH 7.0 and with the crystal structure. The C_ϵ-proton of Tyr322 can be brought within ~3.3 Å of the Mo atom by rotation of the Tyr322 ring plane around the $C_\beta-C_\gamma$ bond by 16°, thereby placing the C_ϵ-proton in the general direction of the **g** tensor axis *1*. Tyr322, a conserved residue in all SO, is hydrogen-bonded to the equatorial Mo−OH group of the active site[1] and has been proposed to play an essential role in the catalytic cycle of SO.[5,33]

Conclusions

In this work, we have recorded and qualitatively analyzed the pulsed ENDOR spectra of the nonexchangeable protons of

(33) Pacheco, A.; Hazzard, J. T.; Tollin, G.; Enemark, J. H. *J. Biol. Inorg. Chem.* **1999**, *4*, 390−401.

the Mo(V) sites of chicken and human SO at pH 7 (lpH) and 9.5 (hpH). The close similarity of the spectra for both organisms suggests that the structures of their Mo(V) sites are nearly identical. The prominent hyperfine interaction observed for lpH SO yields a Mo···H distance of ~2.8 Å that has been assigned to the C_α-proton from Cys185 (chicken SO) or Cys207 (human SO) on the basis of an independent measurement of the hfi anisotropy by C-band ESEEM and on comparison with the X-ray structure of chicken SO.[1] The distance obtained from our ENDOR measurements is ~0.16 Å shorter than that estimated from the X-ray structure at pH 7.8 under high sulfate conditions. Such a difference in distance obtained by different methods is at the margin of distingishability (see Appendix 1) and may not be significant.

In hpH SO, the minimal distance from Mo(V) to the nonexchangeable protons becomes ~3.3 Å. This value is meaningfully different from the X-ray and lpH SO distances and indicates that some structural modification takes place upon raising the pH. The minimum structural modifications that account for such a distance change can be described by two ~15° rotations around $C_\alpha-C_\beta$ and $C_\beta-S_\gamma$ bonds of the coordinated cysteinyl residue that may reflect small pH-dependent changes in the folding of the protein near the active site. The ENDOR spectra of the nonexchageable protons in hpH SO show little dependence on the orientation of $\mathbf{B}_o$ in the molecular frame, which implies that several protons located at $R_{MoH} \approx 3.3$ Å and at various angular positions in the molecular frame are responsible for the main features of the ENDOR spectra of hpH SO. The analysis of the minimal structural variations at the Mo site shows that these protons may include the C_α-proton and one C_β-proton of Cys185 (chicken numbers), one C_γ-proton of Arg138, and the C_ϵ-proton of Tyr322.

Finally, the results of this investigation of the nonexchangeable proton environment of the Mo center in native chicken and recombinant human SO in both the lpH and hpH forms establish the fundamental background for the assessment of structural variations around the Mo center that may occur in mutant forms of SO, even when the mutation is some distance from the active site.

Acknowledgment. We gratefully acknowledge the support of the NIGMS (GM-37773 to JHE and GM44283 to KVR), and we thank the National Science Foundation for funds for construction of the EPR spectrometers (Grants DBI 9604939 and BIR 9224431). We are grateful to Ralph Wiley for assistance in purification of the recombinant human sulfite oxidase.

Appendix 1

Potential Errors in the Mo−Proton Distance Estimates. This work compares the Mo···H distance estimates for the C_α-proton of Cys185 obtained using two different techniques: pulsed ENDOR spectroscopy (for Mo(V) preparations at pH 7.0 and 9.5) and X-ray crystallography (for the Mo(VI) preparation at pH 7.8). To understand which difference in the distance estimates can be considered meaningful, we have to take into account the possible errors in distances determined by these techniques.

The distance estimates from the X-ray structure were based on proton positions deduced from positions of adjacent carbons, assuming the C−H bond length of 1.09 Å and placing this bond in such a way that it would be at a 54.5° angle with the $C-C_\alpha-C_\beta$ plane (in the case of the C_α-proton of Cys185), and its projection on the $C-C_\alpha-C_\beta$ plane would bisect the outer part of the $C-C_\alpha-C_\beta$ angle (see, e.g., Figure 3 for the resulting structures). Such a construction represented a tradeoff between trying to impose an idealized sp^3 hybridization and taking into account the actual X-ray coordinates and bond angles derived from the X-ray structure. Because the actual angles between the carbon hybrid orbitals are slightly different (e.g., for Cys185 the angles $N-C_\alpha-C_\beta$ and $C-C_\alpha-C_\beta$ are ~106.4° and 112.2°, respectively), the estimated position of the proton depended on the choice of the base triangle, $N-C_\alpha-C_\beta$ or $C-C_\alpha-C_\beta$ and, thus, included an inaccuracy of ~0.05 Å. In addition, the positions of protons deduced from the X-ray structure are affected by the uncertainties in the carbon atom positions. For a large molecule-like SO, a reasonable estimate of this contribution to R_{MoH} could be as large as ~0.05 Å. The optimistic estimate of total inaccuracy in estimating R_{MoH} from the X-ray structure is, thus, ~0.1 Å (±0.05 Å).

For ENDOR, we will discuss only the inaccuracies unrelated to the assignment of a particular splitting to any given proton (in the context of the 6 MHz splitting observed at g_2, unrelated to the specific assignment to the C_α- or C_β-protons). The inaccuracy of hfi determined by our ENDOR measurements and simulations is ~±0.1 MHz. For a proton ~3 Å away from Mo, this results in an error of the distance estimate of ~±0.03 Å. There is, however, another important contribution to the possible error in ENDOR distance estimates in this system arising from the fact that the spin density is not completely localized on Mo but is partially redistributed to the Mo ligands and Mo−ligand bonds. If this spin density delocalization proves to be significant, the result may even amount to erroneous structural and chemical conclusions, as was recently demonstrated in a 35 GHz ENDOR study of the "Very Rapid" signal of xanthine oxidase.[34]

To estimate the spin density on Mo (ρ_{Mo}) we can use the ^{95}Mo hfi data obtained for lpH and hpH forms of SO.[35] In both cases, the hfi tensors [A_1, A_2, A_3] were moderately rhombic: [170, 75, 50] MHz (the isotropic hfi constant $a_{iso} \approx 98$ MHz) for lpH SO and [163, 63, 34] MHz ($a_{iso} \approx 87$ MHz) for lpH SO, indicating a certain degree of orbital mixing caused by distorted geometry about the Mo.[1] The theoretical anisotropic hfi tensor of Mo resulting from an unpaired electron in a d orbital is axial, with the coupling constant $|T_\perp|_{theor} = (2/7) \times 151 \approx 43$ MHz.[32] Because we are going to compare this tensor with the experimental ones, we will neglect the rhombicity in the latter, and use the avearge value between the two smaller components as an effective experimental $|T_\perp|_{SOexp}$ (36 MHz in lpH SO and 38 MHz in hpH SO) to be compared with the theoretical value. The spin density ρ_{Mo} can now be estimated as $|T_\perp|_{SOexp}/|T_\perp|_{theor}$. This gives $\rho_{Mo} \approx 0.84$ for lpH SO and $\rho_{Mo} \approx 0.88$ for hpH SO.

An independent estimate of ρ_{Mo} can be obtained from comparison of the hfi parameters of Mo in SO with those found for the species giving the very rapid signal in xanthine oxidase ([A_1, A_2, A_3] ≈ [133, 55, 57] MHz ($a_{iso} \approx 82$ MHz)).[36] For the latter species, ρ_{Mo} was estimated to be ~0.62−0.65, since ~35−38% of spin density was found to be delocalized on a double-

(34) Manikandan, P.; Choi, E.-Y.; Hille, R.; Hoffman, B. M. *J. Am. Chem. Soc.* **2001**, *123*, 2658−2663.
(35) Dhawan, I. K.; Enemark, J. H. *Inorg. Chem.* **1996**, *35*, 4873−4882.
(36) George, G. N.; Bray, R. C. *Biochemistry* **1988**, *27*, 3603−3609.

bonded sulfur ligand.[36,37] Independently, $\rho_{Mo} \approx 0.6$ can be estimated for this case from comparison of the effective anisotropic coupling constant in xanthine oxidase $|T_\perp|_{XOexp} \approx$ 26 MHz with $|T_\perp|_{theor}$). Now ρ_{Mo} in SO can be estimated as $(0.6-0.65) \times |T_\perp|_{SOexp}/|T_\perp|_{XOexp}$, giving $\rho_{Mo} \approx 0.83-0.9$ for lpH SO and $\rho_{Mo} \approx 0.88-0.95$ for hpH SO.

The comparison of the isotropic hfi constants could, in principle, also be used to get the estimates of ρ_{Mo} in SO, but the accuracy of such estimates would arguably be considerably worse than that of the estimates based on the anisotropic hfi. The a_{iso} values are ultimately determined by the densities of the s orbitals on the Mo nucleus, whether induced by spin polarization or by admixture of a 4s orbital into the hybrid orbitals and are sensitive to minute details of the complex structure. In addition, the isotropic hfi constant is at least 1 order of magnitude more sensitive to the variations of the spin density in an s orbital than the anisotropic hfi to the variations of the spin density in a d orbital.[32] Therefore, we will not use here the isotropic hfi to estimate ρ_{Mo} in SO. Summarizing the discussion above, we may conclude that $\rho_{Mo} \approx 0.85$ and $\rho_{Mo} \approx$ 0.9 represent reasonable estimates for the spin densities on Mo in lpH and hpH SO, respectively.

Now let us consider spin densities on the ligands. From the hfi constants determined for the equatorial ^{17}O (in SO[38] and related complexes[39]) and ^{33}S (in related complexes[40]) ligands, we may expect the spin densities on these ligands to be small. If we share the spin density deficit on Mo ($\sim$0.15 for lpH SO) among all the ligands, we obtain a reasonable value of 0.03 per ligand. Using these spin densities (0.03 for each direct ligand and 0.85 for Mo), we can now estimate the scale of corrections to the anisotropic hfi tensor caused by the spin density delocalization to the ligands.

For the molecular structure determined by X-ray crystallography, we find that the anisotropic hfi tensor for the cysteine C_α-proton ($R_{MoH} \approx 2.96$ Å) remains virtually axial, (-2.68, -2.71, 5.39) MHz, with the effective perpendicular component $T_\perp \approx -2.7$ MHz compared to -3.04 MHz obtained for the case of $\rho_{Mo} = 1$. The main axis of this tensor is at the angle $\Delta\theta \approx 0.2°$ to that obtained for $\rho_{Mo} = 1$, or in other words, it remains virtually unaffected. Various other distributions of the spin density deficit over the ligands were also tried (including quite unreasonable situations in which the entire spin density deficit of 0.15 was localized on one ligand), and the minimum possible $T_\perp \approx -2.6$ MHz and the maximum possible $\Delta\theta \approx 5.4°$ were found.

The difference of $\sim$13% in the anisotropic hfi estimates obtained for the cases $\rho_{Mo} = 0.85$ and $\rho_{Mo} = 1$ translates into a correction factor of $\sim$0.96 to the distance estimated from the experimental anisotropic hfi using a point dipole model with $\rho_{Mo} = 1$. We have to note, however, that this correction factor was estimated using model distributions in which the spin density was assumed to be localized in certain proportions on the atoms but not on Mo−ligand bonds. This would be a reasonable approximation if the spin density distribution along a bond had a node somewhere in the middle of the bond. Otherwise, it might be more reasonable to distribute the spin density deficit over the middle of the Mo-ligand bonds. Such a distribution results in a correction factor of $\sim$0.99 for the distance from Mo to the C_α-proton of Cys185. At this limit, the difference between the corrected and uncorrected distances for this proton would be $\sim$0.03 Å, or less than the accuracy of its determination from the X-ray structure! From these considerations, we may conclude that 0.96 represents a lower limit estimate for the possible distance correction factor in lpH SO. Therefore, we will use for the C_α-proton of Cys185 in lpH SO an average correction factor of 0.975, and the uncertainty of $\sim\pm0.015$ in the correction factor will contribute $\sim\pm0.05$ Å to the inaccuracy of the ENDOR distance estimate.

Summing up all mentioned sources of inaccuracies, we may conclude that the difference between the distances from Mo to the C_α-proton of Cys185 in lpH SO obtained from the X-ray structure and from ENDOR should be at least 0.13 Å to be meaningful. It follows that the corrected distance estimate from the experimental value of $T_\perp \sim -3$ MHz in lpH SO, $R_{MoH} \approx$ 2.9 Å, is virtually indistingushable from $R_{MoH} \approx 2.96$ Å estimated from the X-ray structure for the C_α-proton of Cys185.

For hpH SO, in which $\rho_{Mo} \approx 0.9$ and the distance from Mo to the cysteine C_α-proton is $\sim$0.3−0.4 Å greater than in lpH SO, the average distance correction factor is $\sim$0.99, the error related to spin density distribution is $\sim\pm0.03$ Å, and the minimal meaningful distance difference between the X-ray and ENDOR estimates is $\sim$0.11 Å. On the other hand, the meaningful difference between the distances obtained by ENDOR in lpH and hpH SO is $\sim$0.1 Å, since the models for the spin density distributions over the ligands for these systems should be similar.

Appendix 2

Davies ENDOR Simulations. In the calculations, the general expression for ENDOR frequencies derived in ref 41 was used. A typical calculation proceeded as follows. Since we concluded (see text and Appendix 1) that the structure of the Mo site in lpH SO is very close to that obtained by X-ray crystallography, the spatial locations of the three protons (C_α- and the closer C_β-proton of Cys185 and the closer C_γ-proton of Arg138, chicken numbering scheme) in the molecular frame were calculated from the positions of the carbon atoms taken from the X-ray crystallographic data, and their respective hybridizations. For a given trial orientation of the **g** tensor in the molecular frame (see text for the definition), the positions of the protons were transformed from the molecular frame to the **g** frame. The anisotropic hfi of the α-proton of Cys185 was assumed to be axial and oriented with the main axis along the Mo−H vector, but its $T_\perp$ value was varied in narrow limits to provide a better fit to the features with $\sim$6 MHz splitting observed in the ENDOR spectrum at g_2. In effect, such a strategy implied the variation of the Mo−H distance without changing the orientation of the radius vector. The isotropic hfi constant of this proton was also varied within narrow limits, although it always remained close to zero.

(37) Howes, B. D.; Bray, R. C.; Richards, R. L.; Turner, N. A.; Bennett, B.; Lowe, D. J. *Biochemistry* **1996**, *35*, 1432−1443.
(38) Cramer, S. P.; Johnson, J. L.; Rajagopalan, K. V.; Sorrell, T. N. *Biochem. Biophys. Res. Commun.* **1979**, 434−439.
(39) Greenwood, R. J.; Wilson, G. L.; Pilbrow, J. R.; Wedd, A. G. *J. Am. Chem. Soc.* **1993**, *115*, 6−5392.
(40) Wilson, G. L.; Greenwood, R. J.; Pilbrow, J. R.; Spence, J. T.; Wedd, A. G. *J. Am. Chem. Soc.* **1991**, *113*, 3−6812.
(41) Hurst, G. C.; Henderson, T. A.; Kreilick, R. W. *J. Am. Chem. Soc.* **1985**, *107*, 7294−7299.

The justification for the variation of $T_\perp$ of the α-proton of Cys185 was provided by the fact that the X-ray studies were carried out on crystals grown at pH = 7.8 from the Mo(VI) state. Our pulsed ENDOR experiments deal with the Mo(V) state at pH 7.0. Clearly, there might be small structural changes between these two experiments. In addition, the positions of protons deduced from the X-ray structure are affected by the uncertainties in the carbon atom positions and by the assumption of idealized sp^3 hybridization for these carbon atoms. As for the nonzero isotropic hfi, it is also a common situation that a small electron spin density is propagated through σ bonds to a considerable distance.[29]

For other protons, the anisotropic hfi tensors were calculated in the point dipole approximation, assuming all the spin density being localized on Mo (since the corrections to the distance to these nuclei accounting for the spin density delocalization from Mo to ligands did not exceed 2%). The isotropic hfi constant for the C_γ-proton of Arg138 was assumed to be equal to zero, because this residue is not a ligand to the molybdenum. For the C_β-proton of Cys185, we have first assumed $a_{iso} = 0$ MHz. It turned out, however, that the spectra could only be simulated with $a_{iso} \approx 1$ MHz (see Results and Discussion).

The orientation of the magnetic field vector $\mathbf{B}_o$ with respect to the **g** frame was varied by systematically changing its polar (θ_B) and azimuthal (φ_B) angles, and the resonance $B_o$value corresponding to each orientation was calculated from the experimental principal g values and mw frequency. When this $B_o$value fell within the limits of ±5 G around the observation field, the ENDOR frequencies were calculated and added to the ENDOR spectra. The ±5 G limits approximated the individual line width used in the simulation of the field-sweep ESE spectrum obtained with the mw pulses the same as those employed for collecting the Davies ENDOR spectra (90° pulse of 60 ns duration and 180° pulse of 120 ns duration). The resulting stick spectra were convoluted with a Gaussian function (0.3 MHz width between the maximum slope points) and multiplied by the intensity factor $I(\nu) = 4(\nu - \nu_H)^2/(4(\nu - \nu_H)^2 + 2\nu_1^2$, where ν_H is the proton Zeeman frequency, and ν_1 is the mw field intensity in frequency units.[42]

JA0115417

(42) Fan, C.; Doan, P. E.; Davoust, C. E.; Hoffman, B. M. *J. Magn. Reson.* **1992**, *98*, 62−72.